

Half metallic ferromagnetism and optoelectronic characteristics of V doped BaTiO₃ compound: a DFT study

A. Sohail^a, S. A. Aldaghfag^b, M. K. Butt^a, M. Zahid^c, M. Yaseen^{a,*}, J. Iqbal^c, Misbah^c, M. Ishfaq^a, A. Dahshan^{d,e}

^aSpin-Optoelectronics and Ferro-Thermoelectric (SOFT) Materials and Devices Laboratory, Department of Physics, University of Agriculture, Faisalabad 38040, Pakistan

^bDepartment of Physics, College of Sciences, Princess Nourah bint Abdulrahman University (PNU), Riyadh 11671, Saudi Arabia

^cDepartment of Chemistry, University of Agriculture, Faisalabad 38040, Pakistan

^dDepartment of Physics - Faculty of Science - King Khalid University, P.O. Box 9004, Abha, Saudi Arabia

^eDepartment of Physics, Faculty of Science, Port Said University, Port Said, Egypt

The effect of vanadium (V) doping with various concentrations ($x= 12.50\%$, 25% , 50% , 75%) on the physical properties of BaTiO₃ perovskite is examined using the spin polarized theory. The electronic band structure (BS) for both states reveal that all Ba_{0.875}V_{0.125}TiO₃, Ba_{0.75}V_{0.25}TiO₃, Ba_{0.5}V_{0.5}TiO₃ and Ba_{0.25}V_{0.75}TiO₃ compounds are half-metallic ferromagnetic (HMF) materials. The results showed that V play a significant role in the HMF behavior of Ba_{1-x}V_xTiO₃ compound. In addition, the magnetic characteristics confirm the integer values of magnetic moment of all mentioned compounds. In optical properties, reflectivity $R(\omega)$, optical absorption $\alpha(\omega)$, dielectric function $\epsilon(\omega)$, extinction coefficient $k(\omega)$, and refractive index $n(\omega)$ are also calculated. The complete set of optical parameters suggests the use of mentioned material in the visible-ultra violet optoelectronics devices. Based on the half metallic (HM) results of V doped BaTiO₃ is capable for spintronics applications.

(Received June 20, 2021; Accepted October 5, 2021)

Keywords: Half metallic ferromagnetic, Density of states, Magnetic moment, Optical parameters

1. Introduction

During the last decade, HMF materials have been attained main interest because of their use in tunnel junctions, optoelectronics and magnetic devices. Moreover, HMF materials play an important part in spintronics, as these materials comprise two spin states, one spin version exhibit metallic behavior and other spin state behave like semiconductor or insulator. The HMFM compounds such as PtMnSb and NiMnSb Heusler alloys were initially reported de Groot et al [1-4].

Meanwhile, perovskite materials have been widely studied due to their low temperature phase transitions [5]. Since 1945, the main focus of researchers has been on the discovery of ferroelectric properties in a single structure called as ABO₃ perovskites crystals that have several technical applications [6-8]. Barium titanate is of great importance in the microelectronics industry as it has superb ferroelectric and piezoelectric properties, low current loss and high dielectric constant [9-11]. Some useful procedures such as doping were used extensively to improve electronic and dielectric properties of barium titanate [12]. CdTe and ZnTe (Cr, Mn and V doped), metal oxides for example CrO₂ and Fe₃O₄, perovskite alloys La_{0.7}Sr_{0.3}MnO₃, Sr₂FeMoO₆ have been explored hypothetically to study their HMF behavior through DFT. In addition, A₂FeBO₆ (A=Ba, Ca, Sr and B=Mo, Re) also demonstrate the HM behavior [13-15]. Renet *al.* probed the yttrium doped BaTiO₃ solubility combining with the electron compensation, which is synthesized by solid

* Corresponding author: m.yaseen@uaf.edu.pk

state process technique. Alshoaibi *et al.* have examined the effect of Y doping at A and B sites (Ba and Ti) of BaTiO₃ by first principle calculations. The outcomes exhibit the enhancement of dielectric properties [16]. Sanna *et al.* computationally examined the electronic, thermodynamic and optical characteristics of cubic and tetragonal phases of BaTiO₃ by using GW approach. The results predicts the disappearance of ferroelectric ordering [17].

In this article, the physical characteristics of Ba_{1-x}V_xTiO₃ ($x= 12.50\%$, 25% , 50% , 75%) have been examined by full potential linearized augmented plane wave method (FP-LAPW) executed in WIEN2K code [18]. The outcomes suggest the use of this compounds for optical and spintronic gadgets.

2. Computational Method

The WIEN2k code based on FP-LAPW scheme within framework of DFT is used for calculating the physical properties of Ba_{1-x}V_xTiO₃ ($x= 12.50\%$, 25% , 50% , 75%) [19]. To calculate the exchange correlation potential, the PBE-GGA has been used [20]. The electronic configuration for Ba, Ti, O, V, is taken as $6s^2, 3d^2 4s^2$, $2s^2 2p^4$ and $3d^3 4s^2$, respectively. In FP-LAPW method, the crystal unit cell contains two sections: interstitial local and muffin tin portion. In the interstitial part, the potential is extended via the plane wave orbitals, however, in the muffin tin area the premise set comprises of the spherical harmonics like nuclear orbitals. In both region potential is given as:

$$V(\mathbf{r}) = \begin{cases} \sum_{LM} V_{LM}(\mathbf{r}) Y_{LM}(\hat{\mathbf{r}}) & \text{inside sphere} \\ \sum_K V_K e^{i\mathbf{K}\cdot\mathbf{r}} & \text{outside sphere} \end{cases} \quad (1)$$

The unit cell of BaTiO₃ contains unit formula along Wyckoff positions of atoms Ba (0,0,0), Ti (1/2,1/2,1/2), O (0, 0.5, 0.5), (0.5, 0, 0.5), (0.5, 0.5, 0). The atomic radii for V, Ba, Ti and O is 1.34, 2.68, 2.15, and 1.52 Å, respectively. The values of muffin tin radii for Ba, Ti, V and O are 2.3, 2.3, 1.75 and 1.75 (bohr), respectively. The plane-wave development is constrained by setting $R_{MT} \times K_{MAX} = 7$. In addition, 1000 k points are selected in the irreducible Brillouin zone (BZ) [21,22]. Inside the angular momentum expansion $l_{max} = 10$ is selected, while the energy cut off is chosen as - 6.0 Ryd, that divide the core and valence state.

3. Results and discussion

3.1. Electronic properties

The determined spin-up and spin-down BS of Ba_{1-x}V_xTiO₃ at $x= 12.50\%$, 25% , 50% and 75% are demonstrated in Figure 1(a-d). The determined electronic BS of Ba_{1-x}V_xTiO₃ compound at all the mentioned doping concentrations displays HM character due to different behavior of spin up and spin down channels. This variation of electronic BS in both channels demonstrate the HM characteristics at $x=12.50\%$, 25% , 50% , 75% . The calculated HM gaps of Ba_{1-x}V_xTiO₃ compound display an increasing trend from 0.93 to 1.14 eV with the increasing concentration from $x=12.5\%$ to 75% .

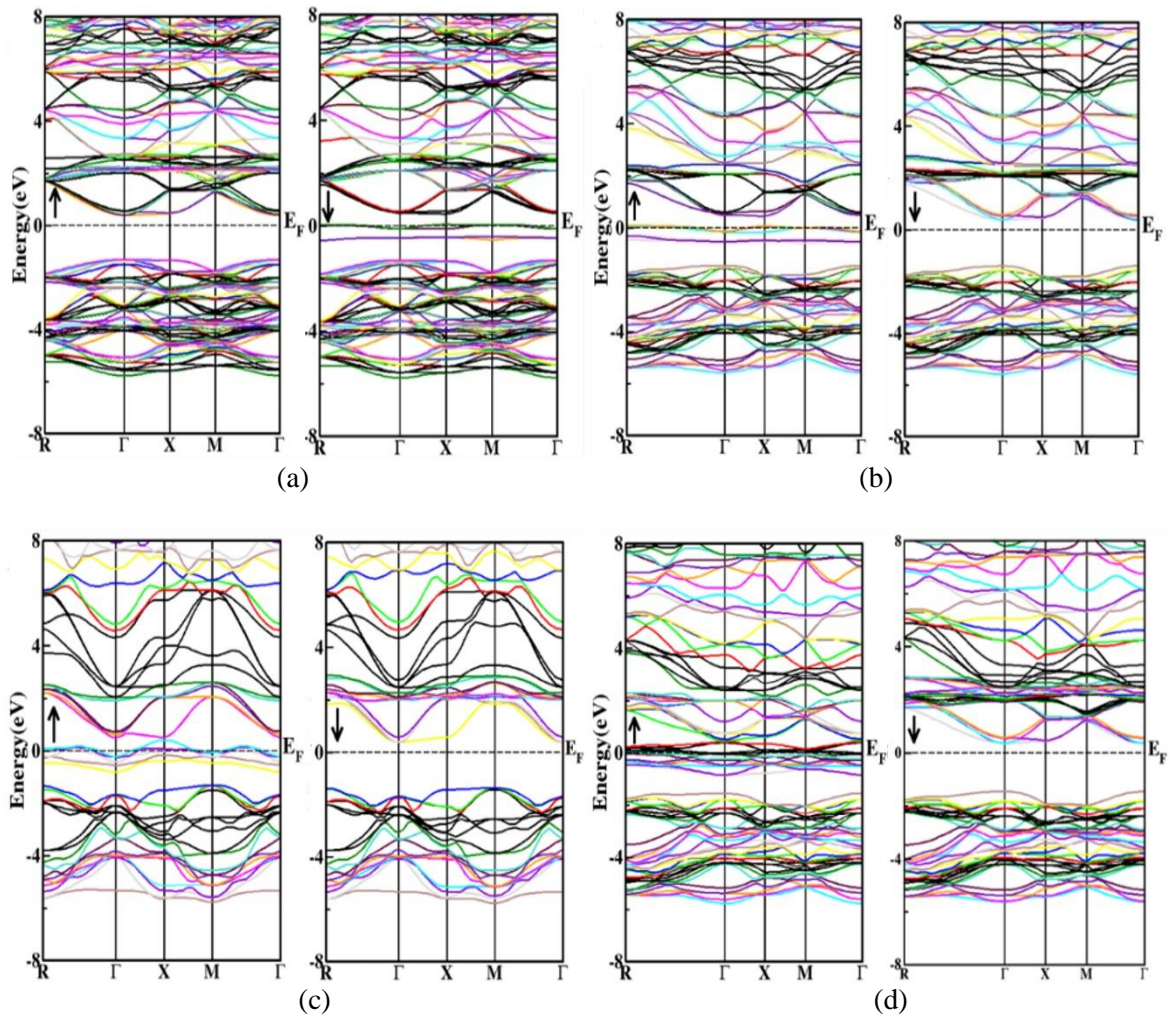


Fig. 1. Spin-dependent BS of V doped BaTiO_3 (a) $x=12.5\%$, (b) $x=25\%$, (c) $x=50\%$, (d) $x=75\%$.

The total DOS of $\text{Ba}_{1-x}\text{V}_x\text{TiO}_3$ at $x=12.50\%$, 25% , 50% , 75% authenticate the HM character, as shown in Fig. 2 (a-d). In order to find out the impact of individual orbitals on the BS, the partial DOS for both spins are represented in Fig. 3 and Fig. 4.

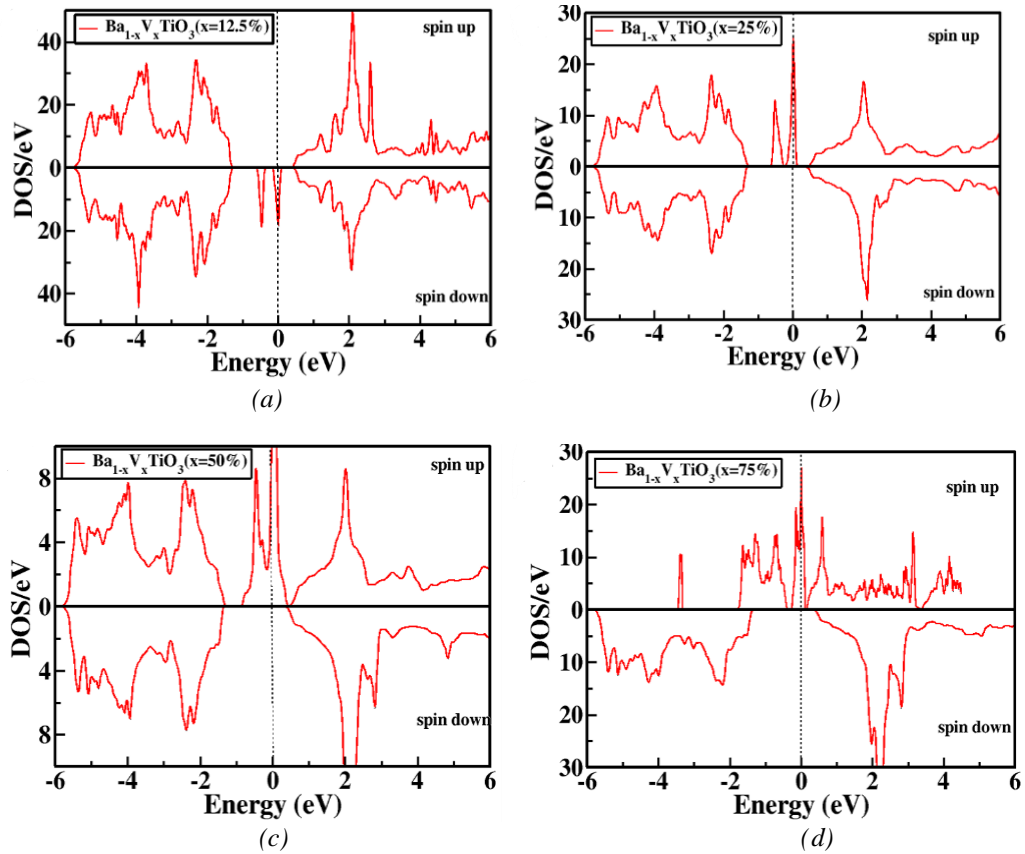


Fig. 2. Spin-dependent TDOS of V doped BaTiO_3 (a) $x = 12.5\%$, (b) $x = 25\%$, (c) $x = 50\%$, (d) $x = 75\%$.

The PDOS is separated in three different regions, such as upper and lower conduction bands (CB) and valence bands (VB). At 12.5% concentration, the TDOS illustrates energy gap of 0.93 eV in spin-upstate and overlapping in the spin-down state. The contribution of V- d and O- p state is maximum in spin down channel in case of VB, while Ti- d has highest contribution in CB for both states. At 25%, 50% and 75%, the spin up channel show metallic behavior because the V- d across the F_E , but, spin down channel demonstrate E_g and major contribution is from O- p state with minor contribution of Ti- d state for both spin channels in case of VB. The CB is largely populated with Ti- d state with minor participation of O- p states, as shown in Figure 4 (b-d).

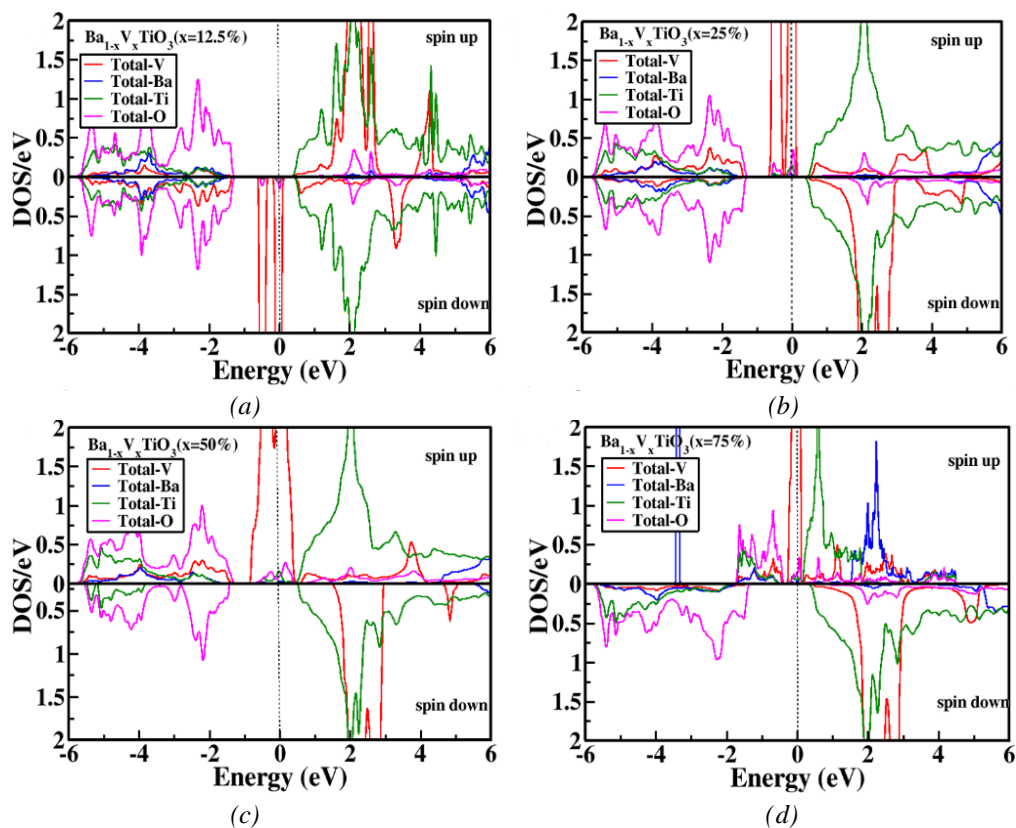


Fig. 3. Spin-dependent TDOS of V doped BaTiO_3 (a) $x=12.5\%$, (b) $x=25\%$, (c) $x=50\%$, (d) $x=75\%$.

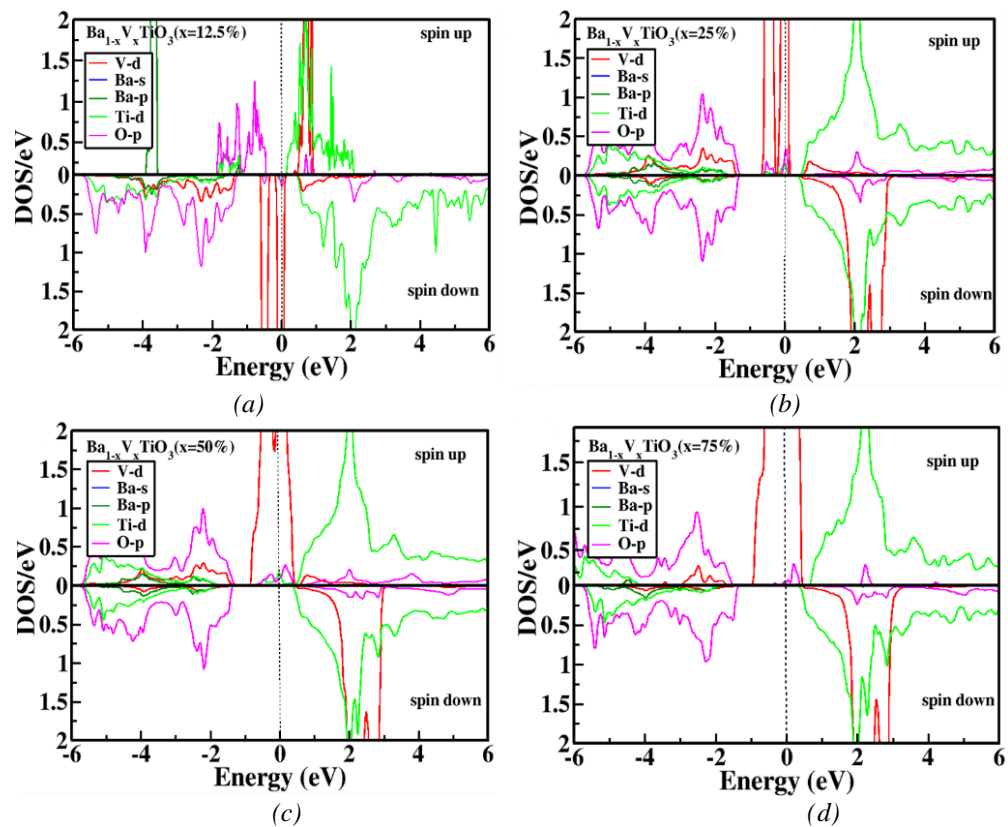


Fig. 4. Spin-polarized partial DOS of V doped (a) $x=12.5\%$, (b) $x=25\%$, (c) $x=50\%$, (d) $x=75\%$.

3.2. Optical properties

The optical response is described in terms of dispersion, polarization, absorption, reflection and conduction. The optical features of the material are revealed by dielectric function and electronic band structure as both are related with one another. The material collaboration to the incident energy is studied by complicated dielectric function, exemplified as $\epsilon(\omega) = \epsilon_1(\omega) + i\epsilon_2(\omega)$ [25,26]. The dielectric function contains real and imaginary parts represented by $\epsilon_1(\omega)$ and $i\epsilon_2(\omega)$, respectively. The absorption of energy capability of material is exhibited by dielectric function's imaginary part. The $\epsilon_2(\omega)$ is computed by direct shift from VB towards the CB. The polarization of the incident light is described by $\epsilon_1(\omega)$. It is mostly derived by the $\epsilon_2(\omega)$ using the relation of Kramers–Kronig [1]. The optical properties of $Ba_{1-x}V_xTiO_3$ at $x= 12.50\%$, 25% , 50% , 75% were calculated.

A schematic of the real part is given in Figure 5a. The maximum peak of dielectric function lies at approximately 0.4 eV for $x= 12.50\%$, 25% and 50% . The maximum value occur at 2 eV for $x= 75\%$. The values of $\epsilon_1(\omega)$ fluctuate with the increment in energy and the negative value is approached at 7 eV. The imaginary part $\epsilon_2(\omega)$ demonstrates the ability of material for absorption of the energy. The highest peaks are shown at 3.68 eV for all concentrations, which illustrate the large absorption in the visible-ultraviolet region, as shown in Figure 5b.

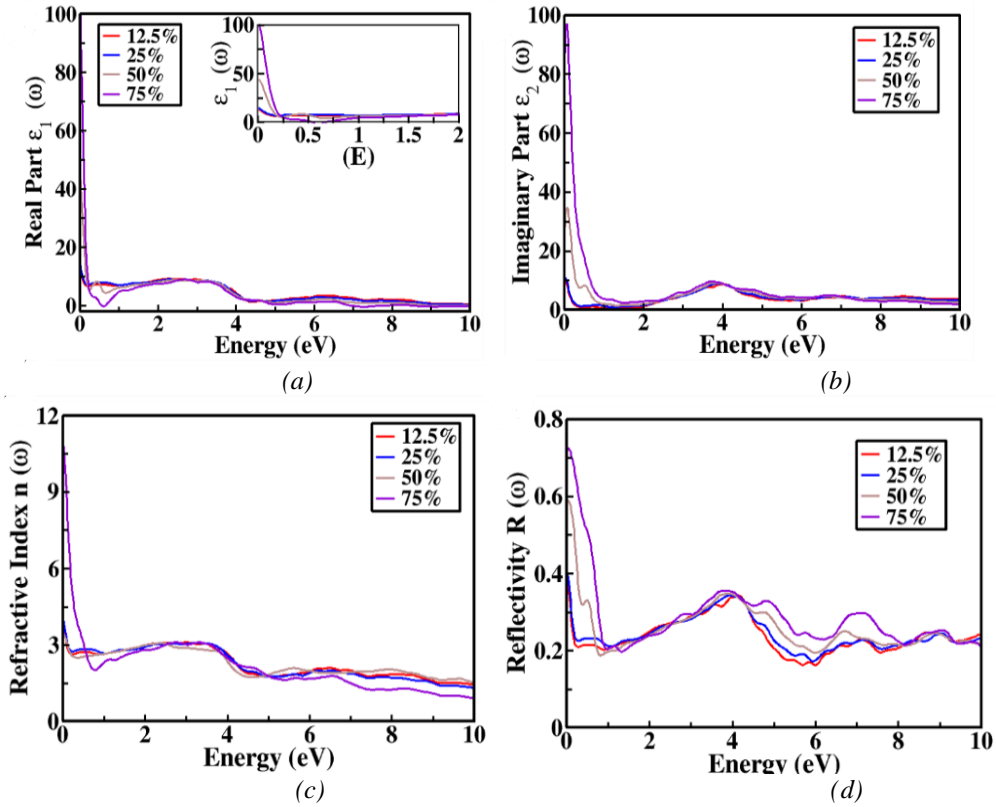


Fig. 5. (a) $\epsilon_1(\omega)$, (b) $i\epsilon_2(\omega)$, (c) $n(\omega)$ and (d) $R(\omega)$ of $Ba_{1-x}V_xTiO_3$ ($x=12.5\%$, 25% , 50% , 75%).

The $n(\omega)$ defines the response of the given compounds to the incident photons. $n(\omega)$ is linked to the $\epsilon_1(\omega)$ and $k(\omega)$ is related with $i\epsilon_2(\omega)$. When the light falls on material's surface the transparency of materials is described by $n(\omega)$. If the substance is extremely translucent, $n(\omega)$ value becomes extremely small (nearly zero) and absorption of light is described by positive values of $k(\omega)$. The maximum values of $n(\omega)$ occur at 3.5 eV for 12.5%, 25%, 50% and 75% concentrations, as shown in Figure 5c. The value of reflectivity is computed by the equation

$$R(\omega) = [n(\omega) - 1]^2 + k^2(\omega) / [n(\omega) + 1]^2 + k^2(\omega) \quad (2)$$

The reflectivity values increases from the zero frequency limit $R(0)$ and the highest value of $R(\omega)$ is occurred at 3.8 eV, as represented in Figure 5d. Moreover, the $k(\omega)$ defines the characteristics of substance to absorb light. The $k(\omega)$ is calculated by the given formula [27]

$$k(\omega) = \alpha\lambda / 4\pi(3)$$

The $k(\omega)$ shows highest peak at 4.0 eV for $Ba_{1-x}V_xTiO_3$ at $x= 12.50\%$, 25%, 50% and 75%, as shown in Figure 6a. The highest peaks of $\alpha(\omega)$ occur among 8.3 eV and 9.1 eV for all given concentrations. The free of charge carriers are represented by the $\sigma(\omega)$. The highest peaks of $\sigma(\omega)$ occur at 8.5 eV, 3.9eV, 3.9eV, 3.86eV for 12.5%, 25%, 50% and 75%, as illustrated in Fig 6c.

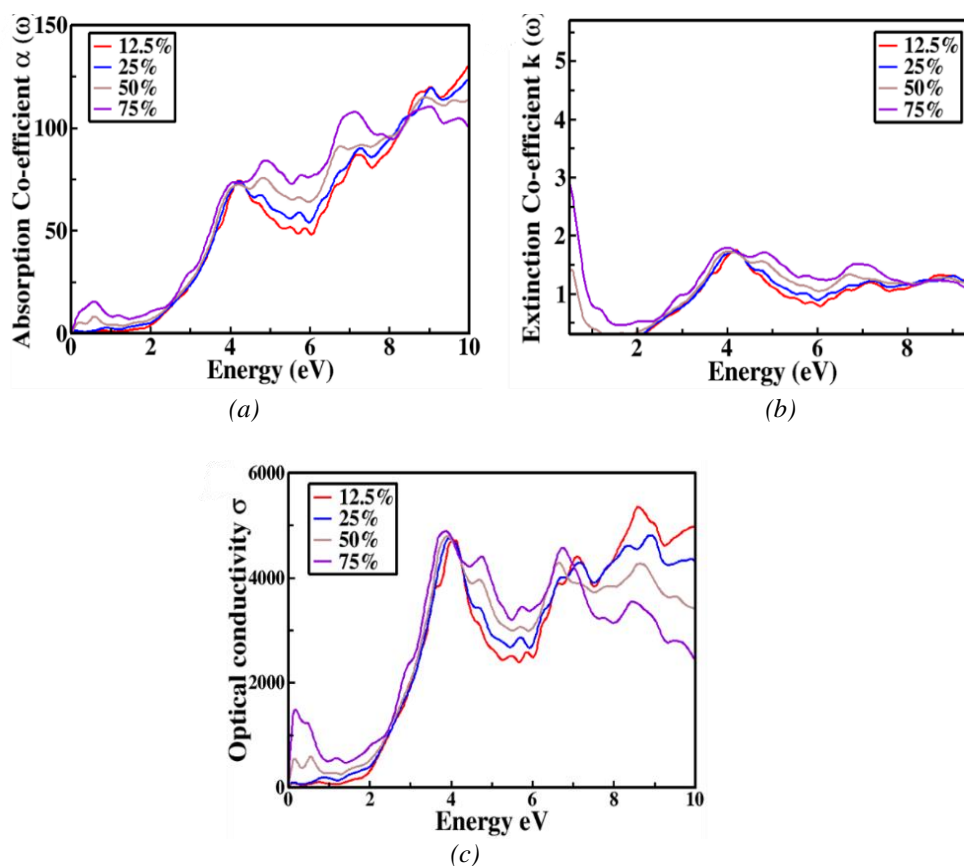


Fig. 6. (a) $\alpha(\omega)$ (b) $k(\omega)$ and (c) $\sigma(\omega)$ of $Ba_{1-x}V_xTiO_3$ ($x = 12.5\%$, 25%, 50%, 75%).

3.3. Magnetic properties

The total, individual and interstitial magnetic moments of $Ba_{1-x}V_xTiO_3$ at $x = 12.5\%$, 25%, 50% and 75% (see Table 1) are computed by using PBE-GGA scheme. The total μ_B of $Ba_{1-x}V_xTiO_3$ at $x = 12.50\%$, 25%, 50%, 75% are 3.00003, 3.00007, 2.99992 and 3.00017 μ_B , respectively. The highest magnetization is observed at $x = 75\%$. The contribution of Ba atoms is weaker as compared to V, Ti and O atoms. Moreover, the direction of the spin configuration is signified by the indication of μ_B of constituent particles. The positive symbol of μ_B of various particles demonstrates that the spins align in a similar way whereas a negative magnetic moment exposes ferromagnetic as well as anti-ferromagnetic collaboration. The μ_B of V, Ba, Ti and O has contrasting signs at 12.5, 25, 50 and 75% concentrations, which shows that V, Ba, Ti and O particles connecting ferrimagnetic state. Therefore, it is evident from the DOS and μ_B outcomes that $Ba_{1-x}V_xTiO_3$ is a HMF compound.

Table 1. The interstitials (M_{int}), atom resolved (M_{Ba} , M_V , M_{Ti} , M_O) and total magnetic moment of V doped $BaTiO_3$ compound.

	M_{int}	M_{Ba}	M_V	M_{Ti}	M_O	M_{tot}
$Ba_{0.875}V_{0.125}TiO_3$	-0.30109	-0.00152	2.73138	-0.01229	0.01125	3.00003
$Ba_{0.75}V_{0.25}TiO_3$	0.29902	0.0023	2.73274	0.02508	0.03389	3.00007
$Ba_{0.5}V_{0.5}TiO_3$	0.30363	0.00208	2.75652	0.04461	0.07882	2.99992
$Ba_{0.25}V_{0.75}TiO_3$	-0.30109	-0.00085	2.73194	-0.00011	-0.00104	3.00017

4. Conclusion

In this $Ba_{1-x}V_xTiO_3$ system, the electronic, magnetic and optical properties are analyzed by PBE-GGA approximation executed in WIEN2K code. The electronic properties and magnetic outcomes present HMF behavior of $Ba_{0.875}V_{0.125}TiO_3$, $Ba_{0.75}V_{0.25}TiO_3$, $Ba_{0.5}V_{0.5}TiO_3$ and $Ba_{0.25}V_{0.75}TiO_3$ compounds, and vanadium is found as the major source of magnetization. The maximum magnetization is observed at $x=75\%$. The optical characteristics such as $R(\omega)$, $\alpha(\omega)$, $\epsilon(\omega)$, $k(\omega)$, and $n(\omega)$ are also computed to probe the optical features of $Ba_{1-x}V_xTiO_3$ for optoelectronic applications. The outcomes illustrate the use of this material for spintronic and visible-ultraviolet optoelectronic devices.

Acknowledgements

This research was funded by the Deanship of Scientific Research at Princess Nourah bint Abdulrahman University through the Fast-track Research Funding Program. The author (A. Dahshan) gratefully thank the Deanship of Scientific Research at King Khalid University for the financial support through research groups program under grant number (R. G. P.2/89/42).

References

- [1] M. K. Butt, M. Yaseen, A. Ghaffar, M. Zahid, *Arabian Journal for Science and Engineering* **45**, 4967 (2020).
- [2] M. Yaseen, H. Ambreen, U. Shoukat, M. Butt, S. Noreen, S. Rehman, S. Ramay, *Journal of Ovonic Research* **15**, 401 (2019).
- [3] Q. Mahmood, M. Hassan, M. Yaseen, A. Laref, *Chemical Physics Letters* **729**, 11 (2019).
- [4] M.K. Butt, M. Yaseen, A. Ghaffar, M. Zahid. *Arabian Journal for Science and Engineering*, **45**(6), 4967-4974 (2020).
- [5] S. Tariq, A. Ahmed, S. Saad, S. Tariq, *Aip Advances* **5**, 077111 (2015).
- [6] N. A. Mazlan, A. F. S. M. Huri, N. A. Zabidi, A. N. Rosli, *Solid State Science and Technology* **26**, 157 (2016).
- [7] R. I. Eglitis, E. A. Kotomin, G. Borstel, S. E. Kapphan, V. S. Vikhnin, *Computational materials science* **27**, 81 (2003).
- [8] A. A. Emery, C. Wolverton, *Scientific data* **4**, 1 (2017).
- [9] C. B. Samantaray, H. Sim, H. Hwang, *Microelectronics journal* **36**, 725 (2005).
- [10] H. Moriwake, *International journal of quantum chemistry* **99**, 824 (2004).
- [11] S. Piskunov, E. A. Kotomin, E. Heifets, J. Maier, R. I. Eglitis, G. Borstel, *Surface Science* **575**, 75 (2005).
- [12] D. Cao, B. Liu, H. Yu, W. Hu, M. Cai, *The European Physical Journal B* **88**, 1 (2015).
- [13] W. H. Xie, B. G. Liu, *Journal of applied physics* **96**, 3559 (2004).
- [14] K. I. Kobayashi, T. Kimura, H. Sawada, K. Terakura, Y. Tokura, *Nature* **395**, 677 (1998).
- [15] G. Vaitheeswaran, V. Kanchana, A. Delin, *Journal of Physics: Conference Series* **29**, 008. IOP Publishing, 2006.
- [16] A. Alshoabi, M. B. Kanoun, B. UIHaq, S. AlFaify, S. Goumri-Said, *ACS omega* **5**,

- 15502 (2020).
- [17] S. Sanna, C. Thierfelder, S. Wippermann, T. P. Sinha, W. G. Schmidt, *Physical Review B* **83**, 054112 (2011).
- [18] F. Shakoor, S. A. Aldaghfag, M. Yaseen, M. K. Butt, S. Mubashir, J. Iqbal, M. Zahid, A. Murtaza, A. Dahshan, *Chemical Physics Letters*, **779**, 138835(2021).
- [19] P. Blaha, K. Schwarz, P. Sorantin, S. B. Trickey, *Computer physics communications* **59**, 399990).
- [20] J. P. Perdew, K. Burke, M. Ernzerhof, *Physical review letters* **77**, 3865 (1996).
- [21] M. K. Butt, Yaseen, M., Iqbal, J., Altowyan, A. Murtaza, M. Iqbal, A. Laref, *Journal of Physics and Chemistry of Solids*, **154**, (2021).
- [22] S. Riaz, M. Yaseen, M. K. Butt, S. Mubashir, J. Iqbal, A. S. Altowyan, A. Dahshan, A. Murtaza, M. Iqbal, A. Laref, *Materials Science in Semiconductor Processing*, **133**, 105976 (2021).
- [23] F. Yang, S. Lin, L. Yang, J. Liao, Y. Chen, C. Z. Wang, *Materials Research Bulletin* **96**, 372017).
- [24] M. Rizwan, I. Zeba, M. Shakil, S. S. A. Gillani, Z. Usman, *Optik* **211**, 164611 (2020).
- [25] S. Al-Qaisi, R. Ahmed, B. U. Haq, D. P. Rai, S. A. Tahir, *Materials Chemistry and Physics* **250**, 123148 (2020).
- [26] O. Tahiri, S. Kassou, R. Mrabet, *Materials and Devices* **3**, 2004 (2018).
- [27] M. K. Butt, M. Yaseen, I. A. Bhatti, J. Iqbal, A. Murtaza, M. Iqbal, A. Laref, *Journal of Materials Research and Technology* **9**(6), 16488 (2020).
- [28] S. Mubashir, M. K. Butt, M. Yaseen, J. Iqbal, M. Iqbal, A. Murtaza, A. Laref, *Optik* **239**, 166694(2021).